Nonlinear Analysis of Individual Quantum Events in a Model with Bohm Trajectories

Kurt Bräuer

Eberhard-Karls-Universität Tübingen, Institut für Theoretische Physik, Auf der Morgenstelle 14, D-72076 Tübingen

Reprint requests to Dr. K. B.; e-mail: kurt.braeuer@uni-tuebingen.de

Z. Naturforsch. **54a,** 663–674 (1999); received September 27, 1999

The quantum mechanical model under consideration describes a particle beam under the influence of an oscillator. Bohm's causal interpretation of quantum mechanics is used to calculate trajectories of the particles. Individual quantum events are defined by the intersection of the beam particle trajectories and the particle detector. The time sequence of individual quantum events is interpreted as a time series and is analyzed by linear and nonlinear methods, which involves reconstruction and investigation of the system in an embedding space. The Fourier amplitudes and the fill factors show white noise, however the Karhunen-Loeve components indicate the influence of the oscillator on the beam particles. In this model individual quantum events carry information which can be detected by the Karhunen-Loeve expansion.

Key words: Individual Quantum Events; Nonlocality; Bohm Trajectories; Time Series; Reconstruction of Trajectories.

PACS: 03.65.Bz; 05.45.Tp

1. Introduction

1.1. Individual Quantum Events

Quantum mechanics (QM) predicts the statistics of many individual quantum events (IQE) in a specific measurement. A particle beam passes for example a slit and hits a screen. The collision of each particle can be observed as a single event. One can exactly predict the pattern on the screen, which is formed by thousands or millions of such events.

The situation becomes confusing, when one tries to understand each IQE. Bohr's interpretation assumes that before observation the quantum system is not part of our reality (Jammer [1]), Heisenberg [2] peaks of a transfer from possibilities to actualities and Pauli (Laurikainen [3]) assumes even irrational influences. Very spectacular are ideas about parallel universes by Everett [4], Wheeler [5] or DeWitt [6]. Recently Rössler [7] presented many arguments for a scenario, where the observer lives in many parallel universes but his consciousness and memory has only part of one at a time.

A rational explanation for the specific appearance of an IQE within QM is given by the causal interpretation of Bohm (Bohm Hiley [8], Holland [9]). This interpretation also suggests a formal way to extend ordinary QM to a causal quantum mechanics (CQM) which allows to some extend even investigations of IQEs. No other interpretation has this possibility at the moment.

1.2. Bohm's Causal Interpretation

By separation of the real and imaginary part of the Schrödinger equation QM can be brought into the form of classical statistical mechanics. What goes beyond classical mechanics is a new kind of a potential, the so called quantum potential. It depends in some way on the curvature of the particle density and is so very different from classical potentials. It causes all the special quantum mechanical phenomena such a state dependence, interference, tunneling and so on.

In Bohm's picture of QM one can define particle trajectories in exactly the way one does in classical mechanics and follow the particles on their way to the detector. This leads to CQM and goes beyond standard QM. In general an IQE is then defined by position and time of the intersection between a particle trajectory and the detector. The statistical behavior of these IQEs is by definition exactly the same as in ordinary QM. CQM however places a theoretical tool at disposal to investigate IQE's under the condition that the statistical rules of QM are valid.

In CQM the degrees of freedom of particles and of the action wave of the Hamilton-Jacobi theory are coupled in a nonlinear way and the particle trajectories show nonlinear behavior. Many authors report on that. Schwengelbeck and Faisal [10] determined the Lyapunov exponent and a entropy of Bohm trajectories. Parmenter and

0932-0784 / 99 / 1200-0663 $ 06.00

Valentine [11], Garcia [12] or Lacomelli [13] investigate their chaotic behavior. Dewdney and Malik investigate chaos in a quantum pinball [14].

All this suggests that methods of analysis from nonlinear dynamics are recommended for the investigation of time series from large numbers of IQE's in CQM. They could reveal hidden correlation within such time series.

The chaotic structure of quantum mechanics due to the dynamically laws of CQM is discussed formally and with help of examples by Dürr, Goldstein, and Zanghi [15]. The same authors showed that also in CQM particle positions are distributed equally as, according to Bohr's statistical law, in normal QM. The reason lies in the random initial conditions of the individual particle trajectories (Dürr et al. [16], Cushing et al. [17]). The randomness is a consequence of missing knowledge. In this case no information can be expected in IQE's.

One has to think about a different situation, where we have more knowledge about the particle trajectories. A particle beam for example could pass by another particle, which is bound by some potential around a fixed location. In CQM one then has to describe the beam particles as wave packages and with random initial conditions for the particle trajectories. The initial conditions of the bound particle are also random. But since this particle is never directly observed, they need not be chosen again, after a beam particle has passed and was observed. The bound particle is moving in the potential on one continuous trajectory, while all the beam particles pass by. This causes a quantum correlation between the IQE's of the beam particles. This correlation is strongly superimposed by the randomness of the beam particles. We want to find a way to reveal this correlation.

1.3. Nonlinear Analyses of Time Series

The basic idea of nonlinear analysis is the reconstruction of trajectories in an embedding space form measurements of one dimensional time series. It was proven by Takens [18] that under idealized mathematical conditions each time series of one component of a complex system contains the full information about all relevant components of the system. The full embedding space trajectories of the complex system can be retrieved by several methods. They can then be characterized by quantities like the Lyapunov-exponent, fractal dimensions or K-entropy (Schuster [19]).

Beyond that the fill factor of Buzug et al. [20, 21] gives qualitative insight into the dynamics behind the embedded trajectories and indicates the optimal parameters for their reconstruction. The Karhunen-Loeve (KL) expansion (Haken [22]) allows to disentangle the main degrees of freedom of the system and to separate them from noise.

The question is now how these methods can be applied on time series from IQE's and whether there is some chance to get new information about quantum processes. For that it seems to be reasonable to study a simple model with idealized conditions.

1.4. Investigation in a Theoretical Model

As a hypotheses one can assume that Bohm's trajectories give a meaningful description of quantum particles. One can further model a simple situation where a particle beam is influenced by some other system, lets say an oscillator. This influence could be transmitted by interaction or entanglement of the wave functions.

The particle beam must somehow be prepared. For a first investigation one can assume that the beam particles leave the source at equal time distances and with identical distribution in space. The explicit start position of a particle trajectory can then be chosen randomly with the probability of the particle density in space. By this the influence of the preparation and of a surrounding quantum system on the explicit particle is treated stochastically.

A fixed time after its emission, the position of the particle on its trajectory is measured. This position is influenced by the randomness of the start position, by the two body quantum state and the explicit oscillator trajectory. (QM averages over all possible oscillator trajectories.) A sequence of beam particle positions defines a time series, which can be analyzed with the nonlinear methods described below. The time series is defined by the sequence of IQE's and the trajectory of these IQE's in an abstract embedding space is reconstructed. The embedding space trajectory should not be mixed up with the particle trajectories.

1.5. Outline of the Paper

First Bohm's causal interpretation of QM and the nonlinear methods for time series are introduced. Then the modeling of a quantum experiment and the application of linear and nonlinear analysis on simulated measurements is described in more detail. The result of the calculation is that the Fourier spectrum of the time series shows only white noise. Also the fill factors show no sign of any underlying low-dimensional dynamics. But the

KL components show clearly the influence of the oscillator on the beam particles.

2. Individual Quantum Events in Bohm's Causal Interpretation of QM

To bring the one particle Schrödinger equation

$$-\frac{\hbar}{i}\partial_t \psi = \left\{-\frac{\hbar^2}{2m}\Delta + V\right\}\psi \tag{1}$$

to the form of classical mechanics, one expresses the complex number ψ in polar coordinates

$$\psi = \mathrm{Re}^{iS/\hbar}, \tag{2}$$

and separates the real and imaginary part of (1). The real part turns out to have the form of the classical Hamilton-Jacobi equation when the phase S is identified with the action function:

$$\partial_t S + \frac{(\nabla S)^2}{2m} + \tilde{V} = 0. \tag{3}$$

The potential $\tilde{V}$ is the sum of the Schrödinger potential V and the so called quantum potential Q:

$$\tilde{V} = V + Q \quad \text{with} \quad Q = -\frac{\hbar^2}{2m}\frac{\Delta R}{R}. \tag{4}$$

The imaginary part of the Schrödinger equation leads to the continuity equation of statistical mechanics

$$\partial_t \varrho + \nabla\cdot(\varrho \boldsymbol{v}) = 0,$$
$$\text{where} \quad \varrho = R^2 \quad \text{and} \quad \boldsymbol{v} = \frac{\nabla S}{m}. \tag{5}$$

Quantum mechanics can now be treated as classical statistical mechanics, however with a new kind of a potential Q. This depends on the curvature of R, that means on the specific form of the particle density $\varrho = R^2$. The interpretation of this potential and the problems with it are extensively discussed, for example by Bohm et al. [8] or Holland [9].

So far the formalism is equivalent to quantum mechanics. But now one can take a pattern from classical mechanics and define the canonical momentum of the quantum particle

$$\boldsymbol{p}(\boldsymbol{x}, t) = \nabla S(\boldsymbol{x}, t) = \hbar \cdot \frac{\mathrm{Re}(\psi(\boldsymbol{x},t))\,\nabla\mathrm{Im}(\psi(\boldsymbol{x},t)) - \mathrm{Im}(\psi(\boldsymbol{x},t))\,\nabla\mathrm{Re}(\psi(\boldsymbol{x},t))}{\psi(\boldsymbol{x},t)\,\psi^*(\boldsymbol{x},t)} \tag{6}$$

when the system is in the state ψ and the particle itself at time t is at the position x. For a given wave function ψ, (6) is a differential equation for stream lines of the quantum particle. Without contradiction to QM one can now assume a well defined start position $\boldsymbol{x}(t_0)$, which has a probability $\varrho(\boldsymbol{x}(t_0)) = \psi\psi^*(\boldsymbol{x}(t_0))$, and one can calculate the intersection of the implied trajectory with a particle detector. This defines the IQE. (The interference effects of QM appear due to the quantum potential.)

If one repeats the play with dice for a start position and calculates trajectories for many particles, one generates a sequence of IQEs, which can be interpreted and investigated as a time series.

This is still not exciting since all what one could discover in such a model is the randomness of the start position, which represents the high dimensional influence of the particle preparation and of the surrounding quantum world. What one can hope to see in an analysis of the time series are influences of further particles on the observed particle. Therefore one has to generalize the formalism to many body CQM, which is straight forward (Bohm Hiley [8], Holland [9]). One finds for the canonical momentum of the particle k

$$\boldsymbol{p}_k = \nabla^{(k)} S = \hbar \frac{\mathrm{Re}(\psi)\,\nabla^{(k)}\mathrm{Im}(\psi) - \mathrm{Im}(\psi)\,\nabla^{(k)}\mathrm{Re}(\psi)}{\psi\psi^*}. \tag{7}$$

The behaviour of Bohm trajectories is sometimes quite astonishing, as Englert et al. called it [23, 24]. They calculated trajectories in interferometers with witch-way detectors. If the split beam crosses itself, the Bohm trajectories do not cross but change the part of the beam. Therefore the which-way detector indicates a particle in one part of the beam but the Bohm trajectory will follow the other part. In this work we will not be confronted with such phenomena of crossing beams.

3. Nonlinear Analysis of Time Series

3.1. Reconstruction of Trajectories

There are several ways to reconstruct the phase space structure of a system from one-dimensional time series. Since the data from our model contain a tremendous amount of noise, time delayed coordinates are recommended. They also are used for the analysis of experimental data (Buzug [20]).

For the analysis we start with a one dimensional time series

$$\{\xi_n = \xi(n\,\Delta T)\}, \quad n \in \{1 \ldots N_{\mathrm{Dat}}\}. \tag{8}$$

N_{Dat} is the number of data points, measured with a constant scanning rate of $1/\Delta T$.

In a first step the time series is gauged and normalized:

$$\xi_n \mapsto \xi'_n = \xi_n - \langle \xi \rangle, \tag{9}$$

where

$$\langle \xi \rangle = \frac{1}{N_{\mathrm{Dat}}} \sum_{n \in \{1 \ldots N_{\mathrm{Dat}}\}} \xi_n$$

and

$$\xi'_n \mapsto \xi''_n = \frac{\xi'_n}{\Delta \xi'_n}, \tag{10}$$

where

$$\Delta \xi' = \sqrt{\frac{1}{N_{\mathrm{Dat}}} \sum_{n \in \{1 \ldots N_{\mathrm{Dat}}\}} \xi'^2_n}.$$

(The inverted commas will be omitted from now on.) The embedded trajectory is then defined by the vectors

$$\boldsymbol{x}_n = \begin{pmatrix} x_n^{(1)} \\ x_n^{(2)} \\ x_n^{(3)} \\ \vdots \\ x_n^{(\dim E)} \end{pmatrix} \equiv \begin{pmatrix} \xi_n \\ \xi_{n+\tau} \\ \xi_{n+2\tau} \\ \vdots \\ \xi_{n+\tau\,(\dim E-1)} \end{pmatrix},$$

$$n \in \{1 \ldots N_{\mathrm{Pnt}}\} \text{ with } N_{\mathrm{Pnt}} \equiv N_{\mathrm{Dat}} - \tau\,(\dim E - 1). \tag{11}$$

τ is the so called delay time and the parameter $\dim E$ is the dimension of the embedding space. N_{Pnt} is the number of points in the embedding space.

3.2. Fill Factor

The parameters τ and $\dim E$ have to be determined before reconstruction. This can be done by the fill factor, as defined and extensively investigated by Buzug et al. [16]. The fill factor is a measure for the volume unfolded by the embedded trajectory. It depends on the delay time τ and the dimension of the embedding space $\dim E$. Buzug points out that the fill factor is an excellent tool to distinguish between time series from chaotic dynamics and from random systems. This quantity also gives a good intuitive impression about some important properties of the embedded trajectory. Some illustrative applications are given in [25].

The fill factor is defined by the mean volume of randomly chosen parallelepipeds in the embedded trajectory. If the delay time τ is too small, these volumes will be small as well. The first local maximum of the mean volume as a function of the delay time τ indicates a proper value for the delay time τ. As a function of the embedding space dimension $\dim E$ the fill factor changes its structure with increasing $\dim E$ as long as a higher dimension brings new information about the dynamics of the system.

As an illustration let us consider a simple harmonic oscillation with

$$\begin{aligned} x(t) &= \cos(\omega t), \\ y(t) &= \dot{x}(t) = -\omega \sin(\omega t) = \omega \cos(\omega t + \pi/2) \\ &= \omega x(t + \pi/2\omega). \end{aligned} \tag{12}$$

The embedded trajectory describes an ellipse. The optimal delay time is obviously $\tau = \pi/2\omega$ since for that both degrees of freedom are well unfolded and the area circumscribed by the ellipse is maximal. The worst choice would be $\tau = \pi/\omega$ with $x(t) = \cos(\omega t)$, $y(t) = x(t+\tau) = -\cos(\omega t + \pi) = -x(t)$), where the area has collapsed and $x(t+\tau)$ is linearly dependent on $x(t)$.

For this oscillator also in higher dimensions the embedded trajectories $x(t)$, $x(t+\tau)$, $x(t+2\tau)$, ..., $x(t+(\dim E-1)\tau)$) can circumscribe only a two dimensional area, the $\dim E$-dimensional volume of this area is zero for $\dim E > 2$. Therefore as a function of $\dim E$ this volume indicates that the oscillator has two degrees of freedom and that the optimal delay time for a reconstruction is $\tau = \pi/2\omega$.

To calculate the fill factor one first determines the indices $r_k^{(j)}$ for $\dim E + 1$ random vertices of each of the N_{vol} volumes:

$$\begin{aligned} r_k^{(j)} &= \mathrm{random}\{1 \ldots N_{\mathrm{Pnt}}\},\ k \in \{0 \ldots \dim E\}, \\ j &\in \{1 \ldots N_{\mathrm{Vol}}\}. \end{aligned} \tag{13}$$

The vectors of the parallelepiped boundaries are then

$$\boldsymbol{d}_n^{(j)}(\tau) = \begin{pmatrix} \xi_{r_0^{(j)}} - \xi_{r_n^{(j)}} \\ \xi_{r_0^{(j)}+\tau} - \xi_{r_n^{(j)}+\tau} \\ \xi_{r_0^{(j)}+2\tau} - \xi_{r_n^{(j)}+2\tau} \\ \vdots \\ \xi_{r_0^{(j)}+\tau\,(\dim E-1)} - \xi_{r_n^{(j)}+\tau\,(\dim E-1)} \end{pmatrix}, \tag{14}$$

$n \in \{1 \ldots \dim E\}$.

The matrix of the difference vectors is

$$\mathbf{M}^{(j)}_{\dim E}(\tau) = \left(\boldsymbol{d}_1^{(j)}(\tau), \ldots, \boldsymbol{d}^{(j)}_{\dim E}(\tau)\right), \tag{15}$$

and one gets the volume of the parallelepiped j as the determinant of $\mathbf{M}$:

$$V^{(j)}_{\dim E}(\tau) = \left|\det\left(\mathbf{M}^{(j)}_{\dim E}(\tau)\right)\right|. \tag{16}$$

The appropriate normalized mean volume is chosen as

$$F_{\dim E}(\tau)=\frac{\frac{1}{N_{\mathrm{Vol}}}\sum_{j=1\ldots N_{\mathrm{Vol}}} V_{\dim E}^{(j)}(\tau)}{\left(\max_{n=1\ldots N_{\mathrm{Dat}}}\{\xi_n\}-\min_{n=1\ldots N_{\mathrm{Dat}}}\{\xi_n\}\right)^{\dim E}}, \quad (17)$$

and the fill factor is finally defined by the logarithm of F:

$$f_{\dim E}(\tau)=\log_{10}(F_{\dim E}(\tau)). \quad (18)$$

3.3. Karhunen-Loeve Expansion

If one generates an embedded trajectory $\boldsymbol{x}(t)=(x_1(t),\ldots,x_N(t))$ from differential equations, each component $x_i(t)$ has a well defined meaning. In the case of the Lorenz attractor for example two components are connected with velocities of a liquid in two different directions of space and another component is connected with heat conduction in the system.

If one reconstructs an embedded trajectory from only one component, as described above, then such a classification is not so simple. The single degrees of freedom of the system do not coincide with the axis of the embedding space. The orientation of the embedded trajectory in the embedding space is more or less random.

This disadvantage can be overcome by a method, which is sometimes called Karhunen-Loeve expansion, or singular value decomposition or bi-orthogonal decomposition. An introduction is given by Haken [22] or Golub and Reinsch [26].

The idea is to find new axes $\boldsymbol{\nu}_k$ for the embedding space so that the projection of the embedded trajectory on each axis is maximal. One finds that the optimal axis $\boldsymbol{\nu}_k$ of the rotated trajectory can be derived by solving an eigenvalue problem

$$\mathbf{R}\,\boldsymbol{\nu}_k=\lambda_k\,\boldsymbol{\nu}_k, \quad k\in\{1\ldots\dim E\}, \quad (19)$$

where the matrix elements R_{mn} of the so called covariance matrix $\mathbf{R}$ are defined by the points of the embedded trajectory $\boldsymbol{x}_n$:

$$R_{kl}=\frac{1}{N_{Pnt}}\sum_{n=1\ldots N_{Pnt}} x_n^{(k)}\,x_n^{(l)},\ k,l\in\{1\ldots\dim E\}. \quad (20)$$

The single degrees of freedom can then be viewed in the time series

$$y_n^{(k)}=\boldsymbol{x}_n\cdot\boldsymbol{\nu}_k. \quad (21)$$

The eigenvalues λ_k are ordered so that $\lambda_k\geq\lambda_{k+1}$, and in addition they sum up to $\Sigma\lambda_k=1$. The larger the value of λ_k is the stronger was the influence of this degree of freedom on the original time series $\{\xi_n\}$.

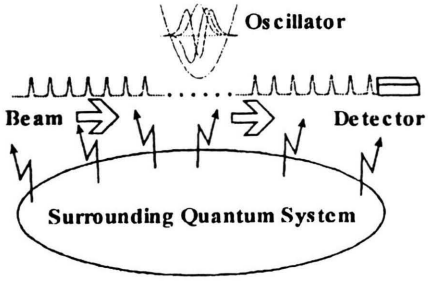

Fig. 1. Setup of the simulated experiment. Beam particles are under the influence of an oscillator and a larger surrounding quantum system. Is there an influence of the oscillator on the beam particles and can this influence be filtered out of the background noise?

4. Generation of Time Series in a Model with Bohm Trajectories

In principle we are interested in a situation as displayed in Figure 1. A particle beam moves under the influence of a surrounding quantum system and on oscillator. The beam particles are detected and a time series is defined by the time distance between the IQEs. We would like to know if we can filter out the influence of the oscillator on the beam if there is only a weak interaction or an entanglement of the wave functions.

A reasonable number of events for nonlinear analysis is about $N_{\mathrm{Dat}}=8000$. The wave function would have to describe all of the 8000 particles plus the oscillator and the surrounding quantum system. Such a system can not be treated in a computer simulation and we therefore consider here a simplified situation.

Let us assume that at times $t=T_N=n\,\Delta T$ well defined particle states ψ_1 are prepared. The influence of the particle history, of the preparation and of the surrounding quantum system determine the specific position of the particle within the distribution of its state. These influences on the beam particle will be treated stochastically in the sense that the particle position is chosen randomly. In case **1** we then assume that the beam particle has a weak local interaction with the oscillator in form of a $W\propto 1/r$ potential. At start time of the simulation the wave functions of both, beam and oscillator particles are not entangled, the two particle wave function is the product of the two single particle wave functions.

In case **2** the wave functions of beam and oscillator particles are entangled. This means that the two particle wave function is not a simple product of two single particle wave functions. This causes a nonlocal interaction between the two particles. The local potential W here is zero.

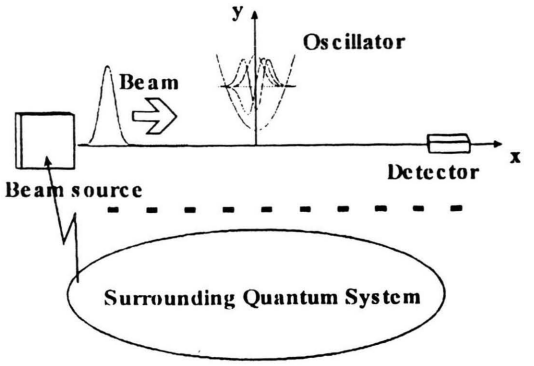

Fig. 2. The situation of Fig. 1 is simplified and reduced to a two body problem. At each time only one beam particle is under consideration together with the oscillator. The influence of the surrounding quantum system and of the preparation of the quantum state is taken into account stochastically in form of the explicit start position $x_1(t)$ of the beam particle. A time series is generated by repetition of the propagation and detection process of single beam particles.

It is always assumed that the wave function is disentangled from the surrounding quantum system due to the preparation of the system and that the extremely weak interaction between the surrounding quantum system with the beam and the oscillator can be neglected during the time of flight ΔT. The system can then be approximated by a two body problem. An illustration is given in Figure 2.

Special care has to be taken on a continuous oscillation of the unobserved particle. At time $t=0$ it is assumed to be in a (finite) Glauber state (Lindner [27]) and its mass is at the position of highest probability. In case **1** then the two body wave function is a simple product wave function, in case **2** the two single body wave functions are entangled as formally described below. At detection of the beam particle the two body wave function is reduced to a pure oscillator wave function which is then taken for the next flight sequence. The position of the oscillator particle is the same at $t=nT+\Delta T-\varepsilon\,(\varepsilon\to 0)$ and $t=(n+1)\,T$, when the next beam particle takes off.

4.1. Wave Function and Time Evolution

A two body wave function can be defined in a two body unitary vector space $\mathsf{U}_2=\mathsf{U}_1^{(1)}\otimes\mathsf{U}_1^{(2)}$ by

$$\Psi(\boldsymbol{x},t)=\sum_{\substack{n_1\in\{0\ldots n_1^{(\max)}\}\\ n_2\in\{0\ldots n_2^{(\max)}\}}} C_{N(n_1,n_2)}(t)\cdot u_{n_1}^{(1)}(x_1)\,u_{n_2}^{(2)}(x_2), \tag{22}$$

where the $u_n^{(1)}$ constitute a basis of $\mathsf{U}_1^{(1)}$ and the $u_n^{(2)}$ of $\mathsf{U}_1^{(2)}$. Furthermore we have

$$N(n_1,n_2)=(n_1+(n_1^{(\max)}+1)\,n_2)\in\{0\ldots N^{(\max)}\} \tag{23}$$

with

$$N^{(\max)}=(n_1^{(\max)}+1)\,(n_2^{(\max)}+1)-1. \tag{23a}$$

The time evolution of the coefficients is

$$C_M(t')=\sum_N \mathrm{e}^{-iH_{MN}(t'-t)/\hbar}\,C_N(t), \tag{24}$$

where the matrix elements of the Hamiltonian $\mathcal{H}$ are defined as

$$H_{MN}=H_{M(m_1,m_2)\,N(n_1,n_2)}=\left\langle u_{m_1}^{(1)}\,u_{m_2}^{(2)}\middle|H\middle|\,u_{n_1}^{(1)}\,u_{n_2}^{(2)}\right\rangle. \tag{25}$$

4.2. Quantities at Time $t=0$

At the start, the coefficients are fixed by

$$C_{N(n_1,n_2)}(0) \tag{26}$$
$$=\begin{cases} c_{n_1}^{(1)}\,c_{n_2}^{(2)} & \text{for case } \mathbf{1} \text{ and}\\ c_{n_1}^{(1)}\,c_{n_2}^{(2)}\,(0.9+0.1\,\delta_{n_2,\,n_1 \bmod n_2^{(\max)}}) & \text{for case } \mathbf{2}. \end{cases}$$

Later we will use Harmonic oscillator wave functions for the $u_n^{(i)}$ and coefficients of Glauber states for the $c_n^{(i)}$. In case **1** the total wave function can be separated into a product of wave functions of particle 1 and 2, in case **2** not. The expression with the Kronecker δ function in (26) entangles the single particle wave functions. The form is very arbitrary. We did not investigate the influence of this specific form on the results of our analysis in detail.

The oscillator start position $x_2(t=0)$ is chosen to be the position of highest probability

$$x_2(t=0)=\langle\Psi(\boldsymbol{x}',t=0)\,|\,x_2'|\,\Psi(\boldsymbol{x}',t=0)\rangle. \tag{27}$$

The start position of the first beam particle $x_1(t=0)$ is chosen with the probability of the corresponding particle density, as described by Knuth [28]:

$$\frac{\int_{-\infty}^{x_1(0)}\int_{-\infty}^{\infty}|\Psi(\boldsymbol{x}',t=0)|^2\,\delta(x_2(0)-x_2')\,\mathrm{d}\boldsymbol{x}'}{\int_{-\infty}^{\infty}\int_{-\infty}^{\infty}|\Psi(\boldsymbol{x}',t=0)|^2\,\delta(x_2(0)-x_2')\,\mathrm{d}\boldsymbol{x}'}=\text{random}\in[0,1]. \tag{28}$$

First the random number is chosen and then the upper limit of the integral is determined as the start position of

particle 1 (beam). By this the distribution of the start positions correspond to the density distributions. For curiosity we also investigate the very special cases, where the start position is the expectation value $x_1(t=0) = \langle x_1 \rangle\ (t=0)$.

4.3. Reduction of the Wave Function at Time $t = nT-\varepsilon$ ($\varepsilon \to 0$) and Quantities at $t=(n+1)\,T$

By detection of the beam particle at the position $x_1(nT-\varepsilon)$, the whole wave function reduces to the wave function of the oscillator

$$\begin{aligned}\Psi^{(2)}(x_2, nT-\varepsilon) &= \sum_{n_1,n_2} C_{N(n_1,n_2)}(nT-\varepsilon) \\ &\cdot u^{(1)}_{n_1}(x_1(nT-\varepsilon))\, u^{(2)}_{n_2}(x_2) \\ &= \sum_{n_2} \tilde{c}^{(2)}_{n_2}(nT-\varepsilon)\, u^{(2)}_{n_2}(x_2). \end{aligned} \tag{29}$$

This defines the coefficients $\tilde{c}^{(2)}_n(nT)$, and the two body coefficients for the next run are

$$C_{N(n_1,n_2)}(nT) \tag{30}$$

$$= \begin{cases} c^{(1)}_{n_1}\tilde{c}^{(2)}_{n_2}(nT) & \text{for case } \mathbf{1} \text{ and} \\ c^{(1)}_{n_1}\tilde{c}^{(2)}_{n_2}(nT)(0.9+0.1\,\delta_{n_2,\, n_1 \bmod n_2^{(\max)}}) & \text{for case } \mathbf{2}. \end{cases}$$

The start position of the next beam particle is then again chosen randomly according to (28), but now with $x_2(nT)$, and the oscillator particle goes on oscillating with

$$x_2(nT) = x_2(nT-\varepsilon). \tag{31}$$

5. Propagation and Oscillation

5.1. Matrix Elements

The Hamiltonian $\mathcal{H}$ is the sum over the beam particle Hamiltonian $\mathcal{H}^{(1)}$, the oscillator Hamiltonian $\mathcal{H}^{(2)}$ and the interaction between them (in case **2**):

$$\mathcal{H} = \mathcal{H}^{(1)} + \mathcal{H}^{(2)} + \mathcal{W}. \tag{32}$$

In harmonic oscillator representation with the basis wave functions

$$u^{(i)}_0(x_i) = \sqrt{\frac{1}{\sqrt{\pi}\, b_i}}\, \mathrm{e}^{-x_i^2/(2b_i^2)} \tag{33}$$

and

$$u^{(i)}_{n_i}(x_i) = \frac{1}{\sqrt{n_i}} \cdot \left\{ \sqrt{2}\,\frac{x_i}{b_i}\, u^{(i)}_{n_i-1}(x_i) - \sqrt{n_i-1}\, u^{(i)}_{n_i-2}(x_i) \right\} \tag{33a}$$

the matrix elements are

$$\begin{aligned} H^{(1)}_{mn} &= \left\langle m \left| \frac{-\hbar^2}{2\,m_1}\,\partial^2_{x_1} \right| n \right\rangle = \frac{\hbar^2}{4\,m_1\,b_1^2} \\ &\cdot \left\{ (2n+1)\,\delta_{m,n} - \sqrt{(n+1)(n+2)}\,\delta_{m,n+2} \right. \\ &\left. - \sqrt{n(n-1)}\,\delta_{m,n-2} \right\} \end{aligned} \tag{34}$$

and

$$\begin{aligned} H^{(2)}_{mn} &= \left\langle m \left| \frac{-\hbar^2}{2\,m_2}\,\partial^2_{x_2} + \frac{1}{2}\,m_2\,\omega_2^2\,x_2^2 \right| n \right\rangle \\ &= \hbar\omega_2\left(n+\frac{1}{2}\right)\delta_{mn} = \frac{\hbar}{m_2\,b_2^2}\left(n+\frac{1}{2}\right)\delta_{mn}. \end{aligned} \tag{35}$$

The particle masses are denoted by m_i, the oscillator lengths by b_i and the angular velocities by $\omega_i = \hbar/(m_i b_i^2)$. For the interaction we assumed a large distance between the particles and get

$$\begin{aligned} W &= \frac{W_0}{|\boldsymbol{x}_1 - \boldsymbol{x}_2|} = \frac{W_0}{|x_1\,\hat{e}_x - x_2\,\hat{e}_x - y_2\,\hat{e}_y|} = \frac{W_0}{y_2} \\ &\cdot \left\{ 1 - \frac{1}{2\,y_2^2}\,(x_1^2 + x_2^2 - 2\,x_1 x_2) + O(x^4/y^4) \right\} \end{aligned} \tag{36}$$

and

$$\begin{aligned} W_{m_1 m_2 n_1 n_2} &= \frac{W_0}{y_2} \\ &\cdot \left\{ \delta_{m_1 n_1}\,\delta_{m_2 n_2} - \frac{1}{2\,y_2^2}\,(\langle m_1 | x_1^2 | n_1 \rangle\,\delta_{m_2 n_2} \right. \\ &+ \langle m_2 | x_2^2 | n_2 \rangle\,\delta_{m_1 n_1} \\ &\left. - 2\,\langle m_1 | x_1 | n_1 \rangle \langle m_2 | x_2 | n_2 \rangle) \right\}, \end{aligned}$$

with

$$\begin{aligned} \langle m | x_i^2 | n \rangle &= \frac{b_i^2}{2} \\ &\cdot \left\{ (2n+1)\,\delta_{m,n} + \sqrt{n(n-1)}\,\delta_{m,n-2} \right. \\ &\left. + \sqrt{n(n+1)(n+2)}\,\delta_{m,n+2} \right\}, \\ \langle m_1 | x_1 | n_1 \rangle \langle m_2 | x_2 | n_2 \rangle &= \frac{b_1 b_2}{2} \left\{ \left(\sqrt{n_1}\,\delta_{m_1,n_1-1} + \sqrt{n_1+1}\,\delta_{m_1,n_1+1}\right) \right. \\ &\left. \cdot \left(\sqrt{n_2}\,\delta_{m_2,n_2-1} + \sqrt{n_2+1}\,\delta_{m_2,n_2+1}\right) \right\}. \end{aligned}$$

y_2 is the distance between beam and oscillator perpendicular to the beam axis (see Figure 2).

Table 1. Parameters of the model calculation. lu are units of length and tu are units of time.

Parameters				
Common				
	action quantum $\hbar$ 1	time integration step width h [tu] .01	particle run time ΔT [tu] 3	
Beam particle				
oscillator length b_1 [lu] 1	mass m_1 [lu^{-2} tu] 1	dimension of space − 1 $n_1^{(\max)}$ 50	mean start position $\langle x_1 \rangle$ [lu] −4	mean start momentum $\langle p_1 \rangle$ [lu^{-1}] 2.5
Oscillator				
Oscillator length b_2 [lu] 2	mass m_2 [lu^{-2} tu] 1	dimension of space − 1 $n_2^{(\max)}$ 2	mean start position $\langle x_2 \rangle$ [lu] −2	mean start momentum $\langle p_2 \rangle$ [lu^{-1}] 0
Interaction	Interaction	time series	embedded trajectories	embedded trajectories
Distance of oscillator form beam axis y [lu] 10	interaction strength case 1, 2 W_0 [tu^{-1} lu] 1, 0	data points N_{Dat} 8000	delay time τ 2	dimension of embedding space dim E 12

5.2. Time Evolution

In the actual calculation, the time evolution operator for the wave function is approximated by the operator

$$U(t) = V^{-1}(t)\, V(-t) = \mathrm{e}^{-iHt/\hbar} + O(t^3)\,, \tag{37}$$

with

$$V(t) = 1 + i\,\frac{Ht}{2\hbar}\,.$$

This operator U is unitary and V^{-1} is easy to evaluate by matrix inversion. It describes small time steps as required for the integration of the particle trajectories. In the case without interaction ($W=0$), however, it factorizes not into single particle operators, as the QM time evolution operator does ($\mathrm{e}^{-i(H_1+H_2)t/\hbar} = \mathrm{e}^{-iH_1 t/\hbar}\ \mathrm{e}^{-iH_2 t/\hbar}$). It therefore entangles the single particle wave functions a little bit during the time evolution. The particle trajectories are calculated with the Runge-Kutta method.

5.3. Glauber States

Glauber states (Lindner [27]) are defined in harmonic oscillator representation by the coefficients

$$c_{n_i}^{(i,\,Glau)}(t) = \frac{\alpha_i^{n_i}}{\sqrt{n_i\,!}}\ \mathrm{e}^{-\alpha_i^2/2}\ \mathrm{e}^{-i\omega_i t/2}\ \mathrm{e}^{-in_i\omega_i t}\,,$$
$$i \in \{1, 2\}\,. \tag{38}$$

They describe states with mean position and canonical momentum

$$\langle x_i \rangle(t_i) = \sqrt{2}\ \alpha_i\, b_i\, \cos(\omega_i t_i)\,,$$
$$\langle p_i \rangle(t_i) = \sqrt{2}\ \frac{\alpha_i}{b_i}\, \sin(\omega_i t_i)\,. \tag{39}$$

Therefore one can chose the expectation values $\langle x_i \rangle$ and $\langle p_i \rangle$ of a state and use the parameters

$$\alpha_i = \pm\sqrt{\frac{\langle x_i \rangle^2 / b_i^2 + \langle p_i \rangle^2\, b_i^2}{2}}\,,$$
$$t_i = \frac{1}{\omega_i}\,\arccos\left(\frac{\langle x_i \rangle}{\sqrt{2}\,\alpha_i\, b_i}\right). \tag{40}$$

6. Parameters and Results

The model parameters for all runs are given in Table 1. No efforts were made to find specially good values. The length b_2 of the oscillator was chosen so that each beam particle reaches the detector within a fraction of the oscillator period time $T_{\mathrm{osc}} = 1/\omega_2$.

The representation space dimension $n_1^{(\max)}$ of the beam particle was chosen to ensure an approximate Gauß form for the beam particle wave function throughout the time

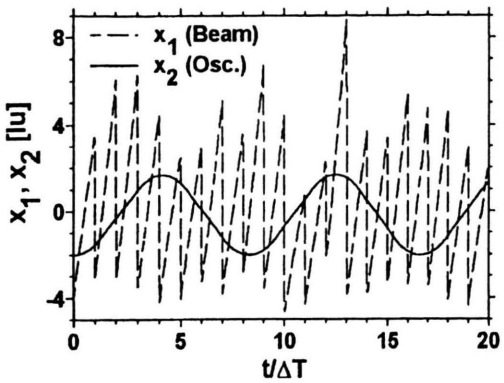

Fig. 3. Trajectories of the oscillator particle (solid line) and beam particles (dashed line) as a function of time. The start position of a beam particle is chosen randomly around a mean position of $\langle x_1 \rangle = -4$ length units [lu]. The particle propagates for a time $\Delta T = 3$ time units [tu]. Then its position is detected and an new particle starts around $\langle x_1 \rangle = -4$ lu. The oscillator goes on oscillating all the time. (The dashed line collects trajectories of 20 beam particles, two of them are always connected.)

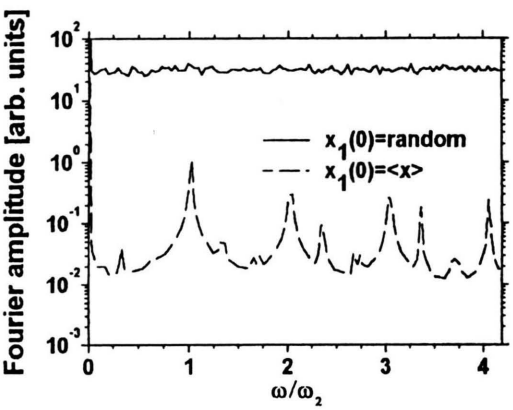

Fig. 4. Averaged logarithm of the Fourier amplitude of a time series. The time series of 4096 points was divided into 16 equal parts and a Fast Fourier Transformation was performed for each part. The frequencies are given in units of the oscillator angle velocity ω_2. The solid line was derived with randomly chosen start positions $x_1(n\Delta T)$ of the beam particles. For the dashed curve it was always $x_1(n\Delta T) = -4$, that means the calculation was completely deterministic. The data of this figure show the result, when an interaction between the beam particles and the oscillator was assumed.

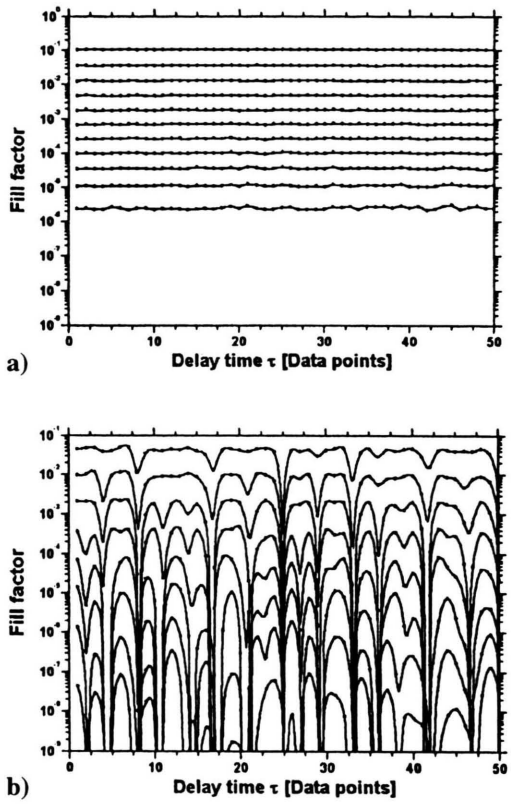

Fig. 5. Fill factors for the reconstructed trajectories of the detection positions. 3 tu after emission the position of each beam particle is determined. The sequence of these positions defines a time series which can be analyzed with nonlinear methods, as described in the text. Figure 5(a) shows the results with stochastically chosen start positions and Fig. 5(b) for the deterministic case (compare explanations to Figure 4).

evolution. The correspondent parameter $n_2^{(\max)}$ for the oscillator was chosen to be as small as possible but allow a stable time evolution. For smaller values of $n_2^{(\max)}$ zeros in the wave function lead to divergences of the trajectories. For the time integration step width h the convergence of the trajectories was tested in the case without noise.

In Fig. 3 we see an example of trajectories for 20 beam particles. The oscillator goes always on oscillating whereas the beam particles jumps after a time period of ΔT to a new, randomly chosen start position. The probability for the start position corresponds to its density distribution (see (28)).

The solid curve in Fig. 4 shows results for calculations with an interaction strength $W_0 = 1$. The logarithmic Fourier spectrum in Fig. 4 is an average over 16 spectra, each covering 256 data points. In other investigations this was found to be a good way to exhibit also very weak structures in the spectrum. Here however we see no structure at all. There is only white noise from the random generator.

Also the fill factor in Fig. 5(a) shows no structure in form of minima or maxima as a function of the delay time

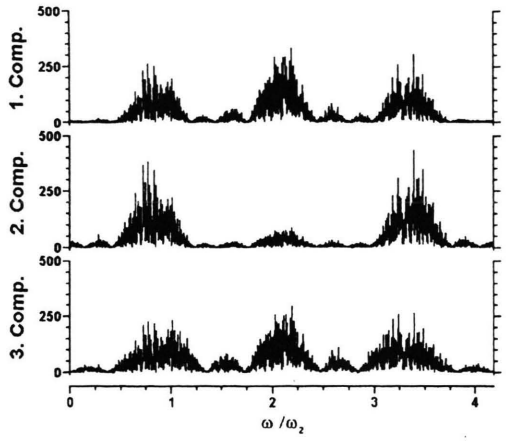

Fig. 6. Fourier amplitudes in arb. units of the first three Karhunen-Loeve components for a calculation with an interaction between the beam particles and the oscillator. A Fast Fourier Transformation was performed for the first 4096 data points of each component. The peaks are tremendously washed out and noisy but they are clearly located around multiples of the oscillator angle velocity ω_2.

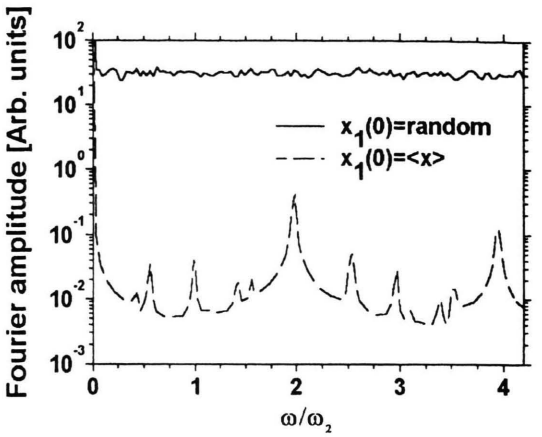

Fig. 7. Averaged logarithm of the Fourier amplitude of a time series as in Fig. 4, but now the particles had no interaction any more. Their wave functions where entangled as described in (26) and (30).

τ. It is important to know that this quantity is very sensible for dynamically influences in a noisy time series and that some authors assume it to be the best known method to uncover such dynamically effects (Buzug [20)].

Only the main components of the KL expansion react on the oscillator influence on the beam particles. This is demonstrated in Fig. 6 in form of the Fourier spectra of the first three KL components. The spectra are calculated from 4096 data points without any averaging and are presented in a linear scale (not logarithmic). They show clear maxima at multiple values of the oscillator angle velocity $\omega_2 = \hbar/(m_2 b_2^2)$.

The first KL eigenvalues are $\lambda_1 = 0.0870$, $\lambda_2 = 0.0870$, $\lambda_3 = 0.0867$. The average eigenvalues is $\langle\lambda\rangle = 1/12 = 0.08333$. This shows dramatically how weak the influence of the oscillator frequency on the investigated time series is compared to the noise and how extremely sensible the KL method is in filtering out the information.

If we switch off the randomness of the beam particle start position and keep all other parameters fixed we find the dashed line in Fig. 4 for the Fourier spectrum and the fill factors in Fig. 5(b). Now the Fourier-spectrum and the fill factors show clearly the dynamics, which is enfolded into the time series.

In the next runs we switched of the interaction between beam and oscillator but entangled the wave functions in a rather arbitrary way, as defined in (26) and (30). The results, shown in Fig. 7 and Fig. 8 are comparable with

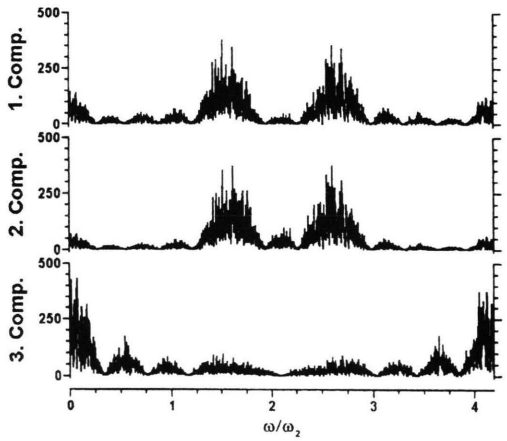

Fig. 8. Fourier amplitudes in arb. units of the first three Karhunen-Loeve components as in Fig. 6, but for the case of entangled wave functions, as described in (26) and (30). The peaks are now located around halve integer values of the oscillator angle velocity ω_2. See the text in Chapt. 6 for an interpretation.

Fig. 4 and Figure 6. Interesting is that now frequencies with half integer multiples of the oscillator are much more pronounced. This can be understood as follows:

The Glauber coefficients of (38) define a QM state which is oscillating as a whole. This is indicated in (39). The individual components of the wave function have no own meaning. This unity is ruined by the entanglement in (26) and (30). Therefore the angle velocities $(n+1/2)\ \omega_2$ of the individual oscillator wave function components $u_n^{(n)}$ show up.

7. Concluding Remarks

The model of this paper shows that on the assumption of Bohm's particle trajectories, information could be enfolded in sequences of IQEs. The detection of these effects is not trivial but the KL-expansion is extremely sensitive and noise resistant so that one can apply this method successfully and hopefully even to data from real quantum measurements.

There arises now of course the question, how different the predictions of CQM in our case are compared to QM. Also in QM the beam particle density should fluctuate at detection time in the rhythm of the oscillator and also this effect should show up in a nonlinear analysis of the IQEs time series. The difference between both theories is that in CQM the influence of one single oscillator trajectory is enfolded in the time series whereas in QM such a trajectory does not exist. A further investigation of this model must show in more detail which difference we can predict between both theories.

One problem of nonlinear analysis, as presented here, is that Taken's reconstruction of embedded trajectories (Takens [18]) requires a constant sampling rate. This of course is an essential handicap, since beam particles usually are not released from the source with equal time distance, as assumed in the model. The realization of exactly this model in the real world would therefore to be not so easy. (The oscillator could eventually be replaced by a LASER.)

However one could apply the analysis method to simpler experimental situations. For example one could take the time between photon emission from atoms as amplitudes of time series or electron emission from a conductor. Do the atomic energy levels or the energy bands show up in the KL-components? The answer of this question could be really exciting.

There might be also other nonlinear methods to detect hidden structures in the noise of IQE's. Freeman [29] for example developed a theoretical model of coupled nonlinear oscillators which is highly sensible on very small influences. Similar to chaos control, small regular influences modify the strange attractor of Freemans dynamically system [30]. Applied to IQE's, the hidden information could show up in form of special space time patterns of a Freeman type system. Such a system could be soft or hard ware. If this works, one would not be restricted to constant sampling rates. (The Freeman model was developed to investigate aspects of the nervous system.)

In this paper nonlocal correlation in a quantum system was investigated. Other kinds of such investigations are experiments of the Einstein-Podolsky-Rosen (EPR) type [31, 32] or of Wheeler's delayed time type [33, 34]. In EPR experiments the nonlocal correlation between two particle is observed by detecting both particles, and in delayed time experiments it is the influence of the observation on one particle. In the approach presented here the influence of system parts on a whole ensemble of detected particles is investigated with the chance of experimental confirmation. The hope is that this leads to a better understanding of individual quantum events.

Acknowledgement

I would like to thank Dr. Bertfried Fauser for many stimulating discussions and for reading the manuscript.

[1] M. Jammer, The Philosophy of Quantum Mechanics; John Wiley & Sons, New York 1974.
[2] W. Heisenberg, Physics and Philosophy; Harper and Row, New York 1958.
[3] K. V. Laurikainen, Beyond the Atom – The Philosophical Thought of Wolfgang Pauli; Springer Verlag, Berlin 1988.
[4] H. Everett, Rev. Mod. Phys. **29,** 454 (1957).
[5] J. A. Wheeler, Rev. Mod. Phys. **29,** 463 (1957).
[6] B. DeWitt, Phys. Today **23,** 30 (1970).
[7] O. E. Rössler, Chaos, Solitons & Fractals **Vol. 7,** 845 (1996).
[8] D. Bohm, B. Hiley, The Undivided Universe; Routledge, London 1993.
[9] P. R. Holland, The Quantum Theory of Motion; University Press, Cambridge 1993.
[10] U. Schwengelbeck and F. H. M. Faisal, Phys. Lett. **A199,** 281 (1995).
[11] R. H. Parmenter and R. W. Valentine, Phys. Lett. **A201,** 1 (1995).
[12] G. Garcia de Polavieja, Phys. Rev. **A53,** 2059 (1996).
[13] G. Iacomelli and M. Pettini, Phys. Lett. **A212,** 29 (1996).
[14] C. Dewdney and Z. Malik, Phys. Lett. **A220,** 183 (1996).
[15] D. Dürr, S. Goldstein, and N. Zanghi, Journal of Statistical Physics **68,** Nos. 1/2 (1992).
[16] D. Dürr, S. Goldstein, and N. Zanghi, J. Statistical Physics **67,** Nos. 5/6 (1992).
[17] J. T. Cushing, S. Goldstein, and A. Fine (eds.), Bohmian Mechanics and Quantum Theory: An Appraisal; Kluwer, Acad. Publ., Dordrecht 1996.
[18] F. Takens, Dynamical Systems and Turbulence, Lecture Notes in Math. **898,** 230 (1980), eds. D. A. Rand and L. S. Young; Springer Verlag, Warwick 1980.
[19] H. G. Schuster, Deterministic Chaos; VCH Verlagsgesellschaft mbH, Weinheim 1989.
[20] Th. Buzug, Analyse Chaotischer Systeme; Mannheim, Bl-Wiss.-Verlag 1994.
[21] Th. Buzug, T. Reimers, and G. Pfister, Europhys. Lett. **13,** 605 (1990).
[22] H. Haken, Principles of Brain Functioning; Springer-Verlag, New York 1996.

[23] B.-G. Englert, M. O. Scully, G. Süssmann, and H. Walther, Z. Naturforsch. **47a,** 1175 (1992).
[24] C. Dewdney and E. J. Squires, Phys. Lett. **A 184,** 6 (1993).
[25] K. Bräuer and M. Hahn, Physics in Medicine and Biology, **44,** Issue 7 (1999).
[26] G. H. Golub, C. Reinsch, Handbook for Automatic Computation, Vol. II, Linear Algebra; Springer-Verlag, Heidelberg 1971.
[27] A. Linder, Grundkurs Theoretische Physik; Teubner, Stuttgart 1994.
[28] D. E. Knuth, The Art of Computer Programming, Vol. **2;** Addison – Wesley, 1974.
[29] W. J. Freeman Biological Cybernetics **56,** 139 (1987).
[30] A. Hoff, Z. Naturforsch. **49a,** 589 (1994).
[31] A. Einstein, B. Podolsky, and N. Rosen, Phys. Rev. **47,** 777 (1935).
[32] A. Aspect, in I. Lingren, A. Rosen, and S. Svanberg (eds), Atomic Physics, Vol. 8; Plenum Press, New York 1983, p. 103.
[33] J. A. Wheeler in A. R. Marlow (ed), Mathematical Foundations of Quantum Theory; Academic Press, New York 1978, p. 9.
[34] J. A. Wheeler, Int. J. Theor. Phys. **21,** 557 (1982).